

Linear DNA for Rapid Prototyping of Synthetic Biological Circuits in an *Escherichia coli* Based TX-TL Cell-Free System

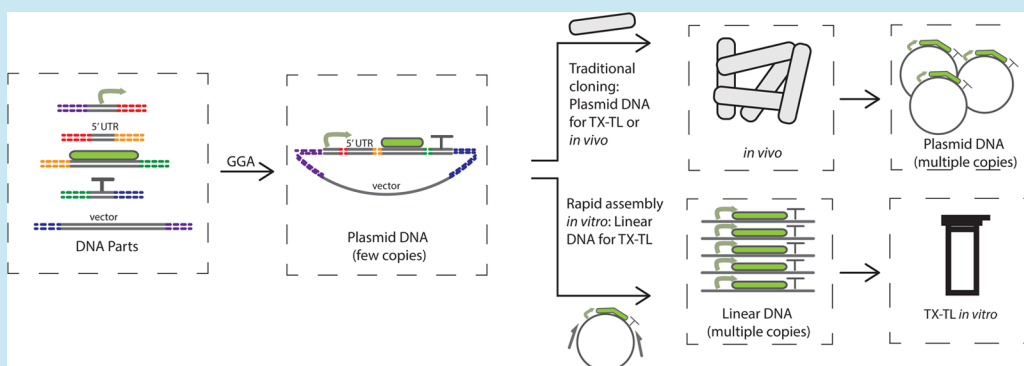
Zachary Z. Sun,^{*,†} Enoch Yeung,[‡] Clarmyra A. Hayes,[†] Vincent Noireaux,[§] and Richard M. Murray^{†,‡}

[†]Division of Biology and Biological Engineering, California Institute of Technology, Pasadena, California 91101, United States of America

[‡]Department of Control and Dynamical Systems, California Institute of Technology, Pasadena, California 91101, United States of America

[§]School of Physics and Astronomy, University of Minnesota, Minneapolis, Minnesota 55401, United States of America

S Supporting Information



ABSTRACT: Accelerating the pace of synthetic biology experiments requires new approaches for rapid prototyping of circuits from individual DNA regulatory elements. However, current testing standards require days to weeks due to cloning and *in vivo* transformation. In this work, we first characterized methods to protect linear DNA strands from exonuclease degradation in an *Escherichia coli* based transcription-translation cell-free system (TX-TL), as well as mechanisms of degradation. This enabled the use of linear DNA PCR products in TX-TL. We then compared expression levels and binding dynamics of different promoters on linear DNA and plasmid DNA. We also demonstrated assembly technology to rapidly build circuits entirely *in vitro* from separate parts. Using this strategy, we prototyped a four component genetic switch in under 8 h entirely *in vitro*. Rapid *in vitro* assembly has future applications for prototyping multiple component circuits if combined with predictive computational models.

KEYWORDS: rapid prototyping, TX-TL, cell-free expression, synthetic biology, biomolecular breadboard, synthetic gene circuits, Golden Gate assembly, rapid linear DNA assembly

The current mode of building synthetic circuits relies heavily on *in silico* design followed by *in vivo* testing and revision. Complete circuits are cloned into a plasmid for propagation *in vivo*, a labor-intensive and serial process that has a 1-week testing cycle, which scales poorly for complex circuits (Figure 1a).^{1–3} Although large-scale successes have been accomplished by this testing method, there is a significant time cost to this engineering cycle. For example, the industrial production of artemisinin from synthetic circuits in *E. coli* and *S. cerevisiae* has taken 150 “person-years,” of which much time can be attributed to part testing.^{4,5}

This current method ignores a commonly applied process in engineering: testing of circuits in a simplified prototyping environment, such as a breadboard, to decrease complexity and increase iteration speed. Cell-free protein synthesis systems are a simplified alternative to *in vitro* systems that are known for ease-of-use and well-defined features.^{6–8} Circuits such as oscillators, switches, and translational regulators^{9–11} have

been implemented either in reconstituted cell-free systems or in S30 extracts.^{12,13} However, these extracts either lack significant similarity to the *in vivo* environment or are optimized for protein production in lieu of circuit design. The ideal cell-free expression system should act as a “biomolecular breadboard” intermediary between circuit testing and *in vivo* implementation. It should mirror the *E. coli in vivo* state while preserving protein production capability and regulatory mechanisms.¹⁴

We propose an S30-based transcription-translation system (TX-TL) that we have developed to serve as part of a biomolecular breadboard. This system is currently supported with characterizations of transcriptional and translational

Special Issue: Cell-Free Synthetic Biology

Received: September 5, 2013

Published: November 22, 2013

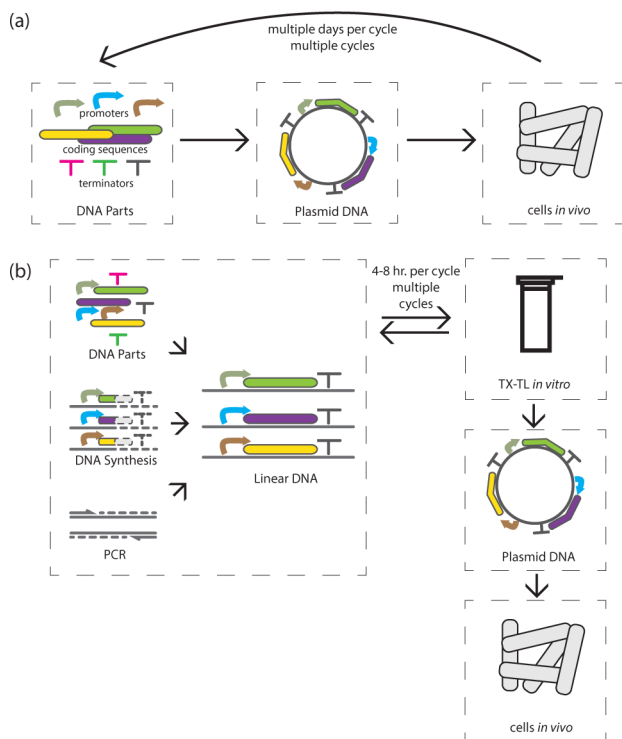


Figure 1. Overview of rapid prototyping procedure of gene circuits. (a) Traditional testing of circuits, where parts are cloned onto a single plasmid or sets of complementary plasmids, tested *in vivo*, and cycled back to construction. (b) Rapid prototyping procedure, where circuits are cycled between construction on linear DNA and testing in TX-TL. When a final circuit prototype is completed, only 1 cycle occurs of plasmid DNA construction and circuit implementation *in vivo*.

processes, computational models, and protocols for its creation and use.^{14–18} We have also demonstrated simple logic gates, cascades, and large-scale assembly of bacteriophage.^{14,19} While most circuits implemented in S30 based extracts utilize plasmid DNA to avoid exonuclease degradation from endogenous RecBCD, linear DNA can be protected from degradation with the RecBCD inhibitor bacteriophage *gamS* protein both *in vivo* and in other S30 extracts.^{20,21} The ability to run circuits off of linear DNA opens up possibilities for rapid prototyping, as linear DNA can be created in high yields either synthetically or entirely *in vitro* in just a few hours. Linear DNA could also enable applications not possible with plasmid DNA, such as the expression and analysis of toxic proteins by bypassing *in vivo* transformation and selection.

In this paper, we established using linear DNA with the biological breadboard for rapid prototyping (Figure 1b). We first developed protective mechanisms to make linear DNA expression comparable to that of plasmid DNA. We also verified recent findings in other S30 extracts which suggested that transcriptional processes using linear DNA are disparate from those using plasmid DNA.²² To validate linear DNA as a prototyping medium, we compared expression of linear DNA to plasmid DNA for a family of promoters and demonstrated similar circuit dynamics for a genetic switch. A rapid, entirely *in vitro* assembly technique was then developed to assemble regulatory elements and basic circuits from standard or custom pieces in under 4 h, with complete testing in under 8 h. By maintaining an engineering cycle time of 8 h or less, our technology theoretically enables prototyping of multicomponent circuits in a standard business day.

RESULTS AND DISCUSSION

Linear DNA Can Be Protected from Degradation in TX-TL. We initially sought to characterize the stability of linear DNA in TX-TL. Integral to this is accurate quantification of both linear and plasmid dsDNA concentration, as large errors in quantifying small amounts of dsDNA can introduce significant downstream bias.²³ This is especially true for TX-TL, as some experiments require less than 10 ng/ μ L of stock dsDNA. Two common methods for dsDNA quantification commonly in use include spectrophotometry and fluorometry. We compared both and established guidelines for measuring linear and plasmid DNA concentrations (Supporting Information S1, Figure S1, Table S1).

Unless otherwise stated, all experiments in the paper were done with a single extract batch to avoid extract-to-extract variation,¹⁴ and DNA sequences used can be found in Supporting Information S2.

To determine ideal conditions for expression of a linear DNA template, we compared the production of fluorescent reporter deGFP from plasmid pBEST-OR2-OR1-Pr-UTR1-deGFP-T500 to that of the 810 bp linear DNA product with no steric protection on the 5' or 3' end. This plasmid was previously optimized for high expression in TX-TL.¹⁶ The deGFP synthesis off of linear DNA was less than 2% that of plasmid DNA (Figure 2a). In order to use lower concentrations of DNA templates for prototyping, we expanded upon previous work, which added purified lambda *gam* in an S30 extract to protect

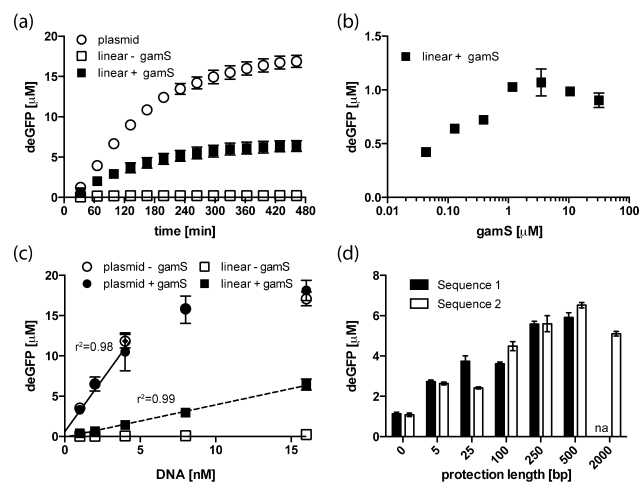


Figure 2. Protection of linear DNA from degradation in TX-TL. (a) Comparison of deGFP time-series fluorescence for plasmid DNA, linear DNA without *gamS* protection, and linear DNA with *gamS* protection. Plasmid DNA used is pBEST-OR2-OR1-Pr-UTR1-deGFP-T500, linear DNA is an 810 bp PCR product with no steric protection ends, and each is supplied at 16 nM. (b) End point deGFP expression after 8 h of 2 nM of linear DNA plotted against signal for different working concentrations of *gamS*, without prior incubation of the protein with crude extract. (c) End point deGFP expression from plasmid and linear DNA with or without *gamS* protein, at increasing DNA concentrations. Correlation of 0.98 on plasmid DNA is for 0–4 nM values only; correlation of 0.99 on linear DNA is for 0–16 nM. (d) Protection of 2 nM of linear DNA using different amounts of noncoding DNA at template ends. Each length corresponds to an amount of noncoding base pairs at each end of the linear DNA, and Sequence 1 is independent of Sequence 2. Readout is end point deGFP fluorescence after 8 h, and experiment is in the presence of *gamS* protein. Error bars represent one standard deviation from three independent experiments.

DNA from exonuclease degradation.²¹ We utilized gamS, a truncated form of lambda gam.²⁰ We also developed a nontoxic storage buffer for use in TX-TL by conducting a toxicity assay of common protein storage buffer additives in an alternate extract (Supporting Information Figure S2, Figure S3). Notably, glycerol as a cryoprotectant is highly toxic to TX-TL and required replacement with DMSO. With gamS protein present in the reaction, deGFP synthesis off of the OR2-OR1-Pr-UTR1-deGFP-T500 linear DNA was 37.6% that of plasmid DNA (Figure 2a).

We determined a gamS working concentration of 3.5 μM by comparing the protective ability of dilutions of purified protein on 2 nM of linear DNA without steric protection (Figure 2b). We used this concentration for subsequent experiments. We hypothesize that 3.5 μM is significantly above saturating levels to inactivate RecBCD, as at 3.5 μM and above the incubation of gamS with crude extract did not improve expression, while below 3.5 μM incubation time improved expression (Supporting Information Figure S4). While purified gamS improved linear DNA expression, it showed no toxicity to plasmid DNA expression (Figure 2c).

We also conducted a saturation curve of plasmid and linear DNA by measuring end point deGFP concentration as a function of DNA concentration. Using this data, we defined a linear regime and saturation regime (Supporting Information Figure S5). The linear regime is defined as the linear region of DNA concentration and output signal, implying little to no resource limitation. In the saturation regime, increased DNA only marginally increases signal. We defined resource limitation broadly as any aspect limiting an *in vitro* reaction, such as polymerase and ribosome saturation or resource depletion (NTPs, amino acids). We ran circuits in the linear regime of DNA concentration to avoid resource limitation affects. While plasmid DNA entered the saturation regime above 4 nM, linear DNA remained in the linear regime up to 16 nM (Figure 2c). This established a typical working concentration for linear DNA and suggested the ability to calibrate linear DNA results to plasmid DNA results by concentration. While much of the discrepancy in saturation can be attributed to promoter strength differences of plasmid versus linear DNA, there may also be contributions from antibiotic resistance cassettes on plasmid DNA diverting resources from the production of deGFP that we did not explore.

With the presence of gamS, we also tested steric protective mechanisms to inhibit degradation by RecBCD and other exonucleases.^{21,24} We first tested two independent noncoding sequences flanking the ends of our linear cassette (Figure 2d). "Sequence 1" was derived from the original plasmid, while "Sequence 2" was from the coding sequences of two long *E. coli* genes, *gltB* and *lhr*, presumed to have no large internal reading frames. Protection was both sequence-specific and length-dependent. Five base pairs (bp) of protective sequences on each end increased signal 2.4-fold over no protective ends. Protection reached a maximum around 250–500 bp, with 6-fold larger signal over no steric protection. Therefore, unless otherwise specified we used 250 bp of protective sequences for subsequent linear constructs. We also tried protecting linear DNA with 1, 2, or 5 phosphorothioate modifications at the 5' end added by PCR, and found improvement only when 5 bp or less of noncoding DNA protection was present (Supporting Information Figure S6a). Interestingly, 5 phosphorothioates on the 0 bp protection construct significantly changed the dynamics of expression, suggesting a minimum protective

length of 15 bp from the –35 promoter region (Supporting Information Figure S6b).

DNA Degradation in TX-TL is Incomplete from the 5' or 3' End. Little is known about degradation patterns of multiple copies of linear DNA in S30 extract-based systems. Knowing whether each copy is selectively degraded at the 5' end or completely removed from the reaction has ramifications for positioning of circuits on linear DNA. To directly measure DNA concentration over the linear regime of a TX-TL reaction, we labeled a typical nonsaturating amount of linear DNA (2 nM, 25 ng) with a fluorescent probe, AlexaFluor-594, in a complementary spectrum to the deGFP reporter. We first incorporated the probe randomly throughout the linear DNA by PCR using an AlexaFluor-594–5-dUTP, which replaced dTTP (Figure 3a). Despite the labeling, linear DNA retained

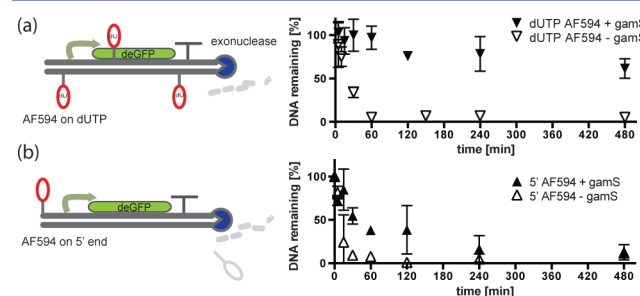


Figure 3. Time-series of DNA degradation in TX-TL at typical working concentrations. (a) DNA degradation of 2 nM (25 ng) of DNA with or without 3.5 μM of gamS. DNA is labeled throughout by an AlexaFluor-594-5-dUTP incorporated by PCR. Percentage of DNA remaining is based on 25 ng present at time 0. (b) Same experiment as panel a, but with AlexaFluor-594 incorporated at the 5' end on a PCR primer. Error bars represent one standard deviation from three independent experiments.

expression ability as measured by deGFP signal. Negligible DNA was degraded within 1 h and over 75% remained within 4 h when templates were protected by gamS, suggesting minimal degradation of template over a typical period of data collection. We also labeled the same template only at the 5' end through PCR by using primers with AlexaFluor-594 covalently bound (Figure 3b). While expression of deGFP was equally conserved, there was significant degradation of AlexaFluor-594 signal as compared to samples labeled throughout the entire linear DNA. We concluded that when gamS and when multiple copies of linear DNA are present, there is incomplete degradation at the 5' end. This is supported by previous data showing only modest expression improvement from increased steric protection lengths (Figure 2d), as well as evidence suggesting the existence of always-active RecBCD complex despite saturating gamS concentration.²⁵ While RecBCD is the primary dsDNA exonuclease, we cannot discount the action of other dsDNA exonucleases such as ExoVII.^{26,27} To our knowledge, this is the first evidence of an exonuclease degradation mechanism with multiple copies of linear DNA.

We also determined that degradation of linear DNA is a saturated process limited by the amount of exonuclease. We conducted the same degradation assay, but using saturating amounts of DNA (250 ng, 20 nM), and saw no significant degradation at 120 min in the presence of gamS (Supporting Information Figure S7). Degradation also seemed invariant to extract preparation conditions. We also made an extract prepared at 29 °C, based on previous work where lower

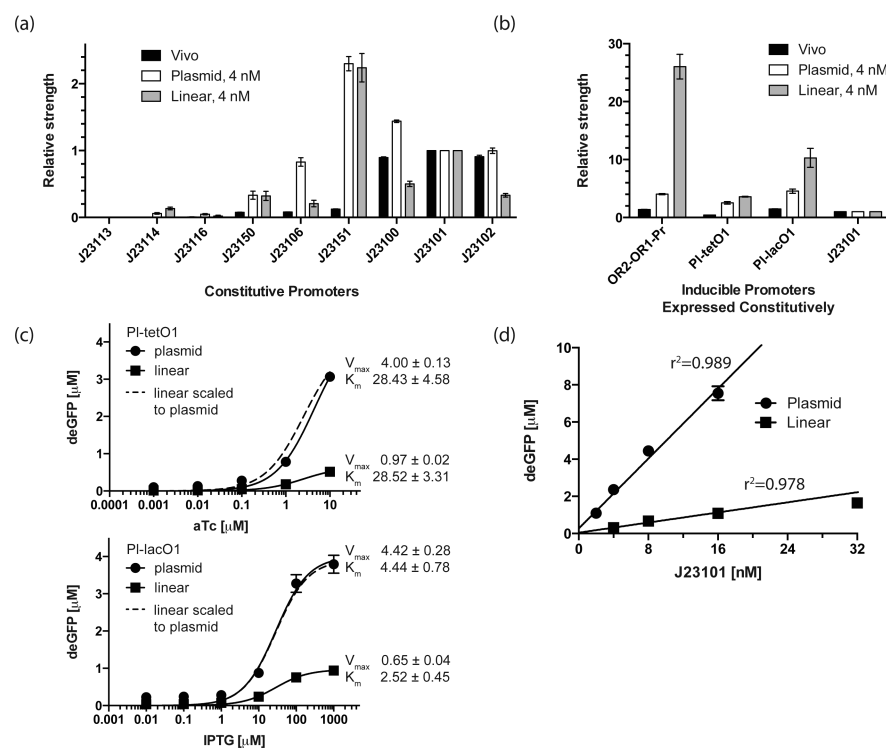


Figure 4. Comparison of different promoter strengths in TX-TL and *in vivo*. (a) Nine commonly used BioBrick promoters are cloned in front of a strong RBS and expressed in either midlog phase *in vivo*, on plasmids in TX-TL, or on linear DNA pieces in TX-TL. Relative end point expression of a 4 nM nonsaturating amount of linear and plasmid DNA is scaled to the strength of J23101, with signal from a random promoter sequence subtracted. (b) Three inducible promoters expressed constitutively are similarly analyzed, scaled to the strength of J23101. For PI-lacO1, 0.5 mM of IPTG is added both to the *in vivo* and the TX-TL data to sequester any native lacI repressor. (c) Hill functions for PI-lacO1 and PI-tetO1 on linear and on plasmid to varying amounts of IPTG and aTc, respectively. Plasmid (1 nM) constitutively producing tetR or lacI is combined with 2 nM of a linear or plasmid reporter. (d) Saturation curve for J23101, plotting end point fluorescence to concentration of linear or plasmid DNA. Both r^2 and linear regression line are derived from 0–16 nM data points. Linear DNA is protected with 250 bp of steric protection and with gamS. Error bars represent one standard deviation from three independent experiments.

preparation temperature decreased exonuclease activity on linear DNA.²⁸ However, we saw no decreased degradation. Based on these findings, we concluded that linear DNA remained present throughout the TX-TL reaction, and could be significantly protected against exonuclease degradation at high concentrations or with sufficient steric protection.

Linear DNA is an Alternative to Plasmid DNA for Circuit Prototyping. Although circuits can be prototyped rapidly using linear DNA, recent studies in other S30 extracts demonstrated a discrepancy between relative expression of linear templates versus plasmid templates.²² These discrepancies were attributed to structural differences between plasmid and linear DNA, as relative activity was recovered by religation of linear DNA and was independent of translation. We hypothesized that, despite structural differences between linear and plasmid DNA, prototyping could still be accomplished by calibrating promoter strength based on DNA concentration between linear and plasmid DNA for constitutive promoters. While a large amount of DNA is needed to obtain signal in other kits, TX-TL allows significant expression for small template concentrations. By working in a linear regime, circuits can be executed such that large amounts of free polymerases and ribosomes exist at all times (Supporting Information Figure S5).

We tested twelve commonly used σ -70 based promoters and a negative control of random DNA for *in vitro* plasmid strength, *in vitro* linear DNA strength, and *in vivo* strength. Linear DNA was protected with gamS protein and 250 bp of noncoding

DNA on either end. Nine promoters are minimal sigma-70 promoters from the Biobrick parts library (<http://parts.igem.org/>), while three are inducible and well-characterized.^{29,30} These constructs all identically expressed deGFP downstream of an untranslated region containing a strong RBS “UTR1.”¹⁶ When each Biobrick promoter was compared in the linear regime and normalized to J23101, there was no correlation between results *in vivo* and in TX-TL either on plasmid or on linear DNA. (Figure 4a). However, when data was taken at highest concentrations measured there was a correlation, if limited, between results *in vivo* and in TX-TL on plasmid DNA (Supporting Information Figure S8). Supporting Information Figure S8 results are similar to a panel done previously in a separate S30 extract, albeit with a different reporter, weaker RBS, different plasmid, and different temperature.²² More work needs to be done to reconcile both data sets, although these results suggest that circuits tested in saturated phase on plasmid DNA most accurately represent the *in vivo* environment. In the *in vivo* environment, we speculate high copy plasmids on strong promoters may reach saturated phase expression. Each inducible promoter was also tested constitutively with the repressor inactivated or not present, and limited correlation was found between *in vivo* results and TX-TL results (Figure 4b). Interestingly, inducible promoters seemed to have vastly stronger strength relative to the minimal sigma-70 based promoter panel in TX-TL.

For the PI-tetO1 and PI-lacO1 promoters, we also characterized the response in TX-TL of linear and plasmid

Table 1. Calibration Data for Different Promoters in TX-TL^a

promoter name	plasmid DNA (P)			linear DNA (L)			P:L ratio
	linear regime DNA [nM]	r^2	m	linear regime DNA [nM]	r^2	m	
OR2-OR1-Pr	0–4	0.998	2.211 ± 0.058	0–8	0.979	1.582 ± 0.018	1.40
Pl-tetO1	0–8	0.980	1.187 ± 0.029	0–16	0.993	0.228 ± 0.029	5.21
Pl-lacO1	0–4	0.990	2.666 ± 0.111	0–8	0.998	0.722 ± 0.085	3.69
J23113	nd	na	na	0–8	0.976	0.003	na
J23114	0–16	0.985	0.025 ± 0.001	0–16	0.981	0.012	2.08
J23116	0–16	0.975	0.022 ± 0.001	0–16	0.984	0.004	5.50
J23150	0–16	0.986	0.187 ± 0.009	0–16	0.982	0.022 ± 0.001	8.50
J23106	0–8	0.992	0.420 ± 0.007	0–16	0.996	0.018	23.33
J23151	0–8	0.982	1.091 ± 0.108	0–8	0.995	0.186 ± 0.017	5.87
J23100	0–8	0.995	0.761 ± 0.049	0–8	0.998	0.041 ± 0.006	18.56
J23101	0–16	0.989	0.470 ± 0.017	0–16	0.978	0.068 ± 0.005	6.91
J23102	0–16	0.976	0.398 ± 0.018	0–16	0.986	0.024 ± 0.003	16.58

^aTwelve promoters are tested at different concentrations in linear (4–32 nM) and plasmid (2–16 nM) DNA form and a linear regime is determined based on a cutoff of $r^2 > 0.975$. The slopes (m) are of the resulting linear regression, in units of μM deGFP/nM DNA. P:L ratio is the ratio of the slopes. nd: signal not detectable. na: not applicable. Error represents one standard deviation from three independent experiments.

DNA to varying amounts of inducer in the presence of repressor (Figure 4c). Data was fit to a Hill function with a Hill coefficient of unity (Supporting Information S3). Operator binding dynamics were similar, with a Michaelis–Menten binding coefficient within two standard deviations for Pl-tetO1 and within one standard deviation for Pl-lacO1. Data for Pl-tetO1 may be biased, however, as TX-TL showed toxicity at values above 10 μM aTc, which seemed to be below saturation phase. We assumed that for Pl-tetO1 and Pl-lacO1, repression binding and unbinding was similar for linear and plasmid DNA at individual operator site.

To calibrate linear DNA to plasmid DNA for constitutive expression, we tested each promoter at different concentrations. Based on the results of end point expression, a saturation curve was produced for both linear and plasmid DNA, where expression was plotted as a function of DNA concentration (Figure 4d). We used a cutoff of $r^2 > 0.975$ to determine a linear regime for each promoter (Supporting Information Figure S9). This data was used to develop a calibration table for linear and plasmid DNA, where the slope of the linear regression line indicated promoter strength in the linear regime (Table 1). A Plasmid/Linear (P:L) ratio was also determined. All promoters were stronger on plasmid DNA than linear DNA, ranging from 1.40 to 23.74 fold. The carrying capacity of TX-TL was capped at 15 μM . However, independent of promoter strength all constructs approached the saturating regime at 32 nM of linear DNA. This suggested a theoretical limit of DNA carrying capacity independent of absolute signal strength, but we were unable to test concentrations above 32 nM for linear DNA or 16 nM for plasmid DNA.

To demonstrate the ability to prototype circuits using either plasmid or linear DNA, we built a 4-piece genetic switch with 2 fluorescent outputs, deGFP and deCFP (Figure 5).³¹ Linear DNA constructs were derived from plasmid DNA by PCR, and had *gamS* present as well as 250 bp of steric protection; 2 nM of each reporter and 1 nM of each repressor were used. We then examined the dynamics of the genetic switch by plotting the end point expression values at 36 different combinations of IPTG and aTc inducers. When both deGFP and deCFP were scaled for equivalent expression, the genetic switch behaved as expected with deGFP expression at high IPTG and deCFP expression at high aTc. As predicted, expression from linear DNA at similar concentrations was also lower than for plasmid

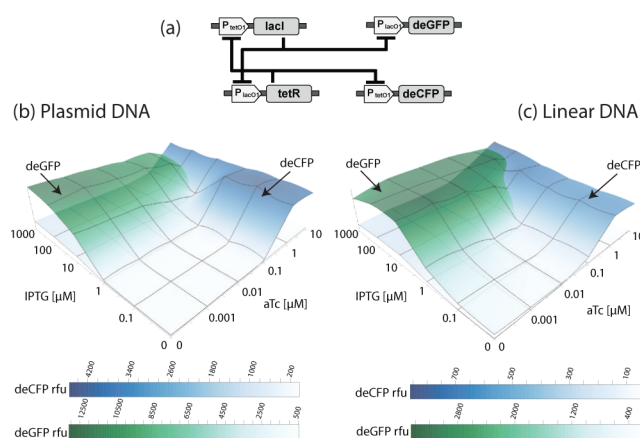


Figure 5. Comparison of a genetic switch made from linear vs plasmid DNA. (a) Diagram of the genetic switch. (b) End point fluorescence of deGFP and deCFP for plasmid DNA at various IPTG and aTc inducer concentrations. Four plasmid DNA pieces are used at 2 nM reporter and 1 nM repressor. Due to the logarithmic scale, 0 μM is represented as 0.01 μM for IPTG and 0.001 μM for aTc. (c) End point fluorescence for four linear DNA pieces at the same concentration. Linear DNA is protected with 31 bp of steric protection and with *gamS*.

DNA. Based on this result, we believe linear DNA prototyping is a viable alternative to plasmid DNA prototyping.

Linear DNA Can Be Rapidly Assembled for Prototyping Circuits. After establishing linear DNA circuit prototyping, we sought to create a method for rapid assembly of linear pieces that would enable us to go from assembly to testing in 4–8 h and simultaneously allow us to generate plasmid DNA post-transformation (Figure 6a). Unlike other *in vivo* assembly methods, which ultimately require efficiency as well as selectivity, we were primarily concerned with selectivity as our templates would be end amplified by PCR. We also favored rapid cycle times in linear DNA to modularity postconstruction, which has been shown to speed up the design cycle *in vivo*.³² We initially tested three methods of *in vivo* assembly for adoption purely *in vitro*: isothermal assembly, chain reaction cloning, and Golden Gate assembly.^{2,33,34} Each method is based on a different mechanism of action—recombination-based cloning, blunt-end cloning, or sticky-end cloning. Of these

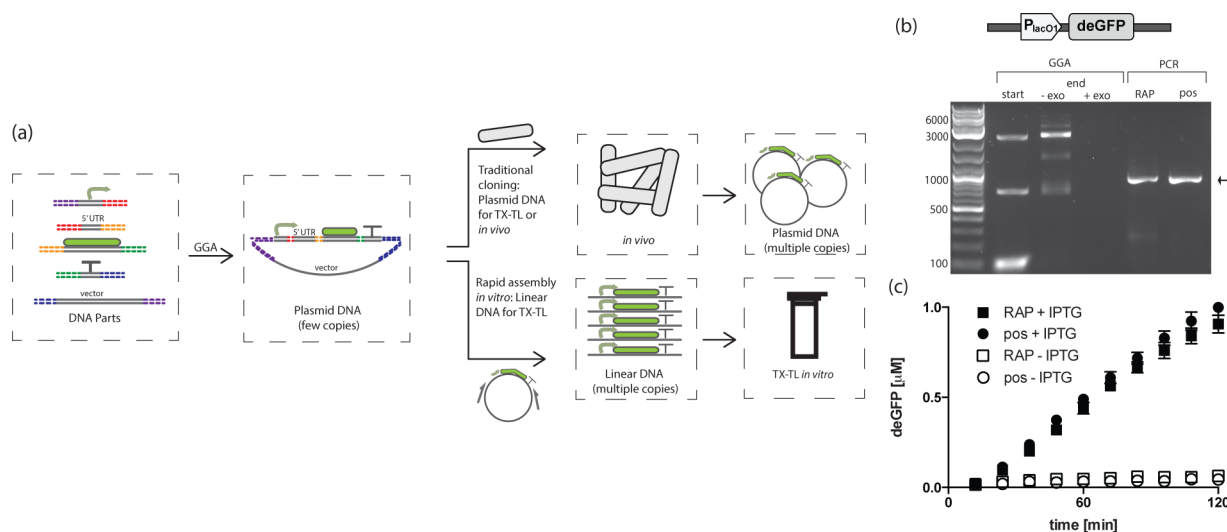


Figure 6. Rapid *in vitro* assembly and prototyping in TX-TL. (a) Overview of the rapid assembly and prototyping procedure, where DNA parts are assembled using Golden Gate assembly (“GGA”) to create a plasmid, which is then directly used as a PCR template to create linear DNA at high concentrations suitable for TX-TL. In parallel, the assembly product can also be propagated *in vivo* to yield more copies of clonal plasmid. Time comparisons for both methods can be found in Supporting Information Table S2. (b) Agarose gel of a gene assembled from 5 standard pieces of 66 bp, 103 bp, 110 bp, 707 bp, and 2376 bp. Shown are 50 ng each of starting fragments (except 66 bp), fragments postassembly before and after exonuclease digestion (“exo”), and rapid assembly PCR product (“RAP”) compared to postcloned PCR product (“pos”). Arrow indicates expected size of 892 bp. (c) Functional testing of 4 nM of rapid assembly or postcloned products, with or without 0.5 mM IPTG inducer. Experiment conducted in the presence of 2 nM Pl-tetO1-lacI linear DNA. Linear DNA is protected with 31 bp of steric protection and with gamS. Error bars represent one standard deviation from three independent experiments.

three, only isothermal assembly and Golden Gate assembly produced enough yield to obtain constructs.

We first assembled a common network motif, a negatively autoregulated gene,³⁵ from 4 linear parts using both isothermal assembly and Golden Gate assembly (Supporting Information Figure S10a). The assembly products were PCR amplified directly afterward to produce rapid assembly products ready for prototyping in TX-TL. The assembly product was also transformed, cultured, purified, and amplified by PCR to produce a positive control. All constructs were sequenced before testing in TX-TL. When run on an agarose gel, rapid assembly products were of the expected size when compared to a post-transformation positive control, with higher than 95% purity (Supporting Information Figure S10b). However, while all constructs showed responses to aTc induction some demonstrated significant background activity (Supporting Information Figure S10c). We hypothesized that a nonspecific product caused by mis-ligation could significantly bias results. To counteract this, we developed a standard assembly procedure based on Golden Gate assembly. By using a standard assembly, any mis-ligation would be less likely to lead to mis-assembled products capable of expression.

Our standard Golden Gate assembly procedure also allowed us to recycle commonly used parts and to ensure functional activity of the desired product. Our standard consisted of five pieces—a promoter, 5' untranslated region (UTR), coding sequence, terminator, and vector (Supporting Information Figure S11). It was designed to be compatible with previously used noncoding sequences and primers on the pBEST vector backbone. We revised a pre-existing standard for use in TX-TL by creating 4 bp binding overhangs with increased specificity.³⁶ Using different overhangs with little overlap was necessary, as we found decreased specificity with multiple base pair overlaps. We also designed our PCR primers to overlap at the junction sites of vector and promoter and vector and terminator,

respectively, which further minimized nonspecific products. This decreased steric protection ends to 31 bp.

Using our standard with pre-made pieces, we rapidly prototyped a Pl-tetO1-deGFP construct and demonstrated functional equivalency in less than 5 h (Figure 6b, c). A detailed time frame with comparisons to testing using plasmids post-transformation is in Supporting Information Table S2. While the assembly reaction did not produce significant amounts of plasmid, a fragment corresponding to the expected size could be amplified. Cleaner PCR products of the assembly reaction were produced by minimizing template concentration and by using overlapping PCR primers (Supporting Information Figure S12). Existing nonspecific products could also be predicted based on size and gel mobility shifts. We have since tested multiple assemblies using our rapid assembly standard and found that correct equimolar ratios of starting products are also essential to isolating a clonal product.

For more complex circuits, we verified our rapid assembly procedure by repeating the construction of the genetic switch in Figure 5a but from rapid assembly products (Supporting Information Figure S13a). Specific bands were formed from PCR off of the rapid assembly product, and TX-TL runs demonstrated similar results for the product and the positive control when responding to IPTG and aTc (Supporting Information Figure S13b, c). This prototyping took under 7 h of time.

Linear DNA Prototyping Theoretically Allows for Large Circuits to Be Tested in a Single Business Day. Our work is primarily focused on the technology development of a rapid prototyping procedure using linear DNA in TX-TL. Therefore, we chose only to demonstrate proof-of-concept assemblies using simple circuits. However, the real return of linear DNA prototyping is in testing large circuits in TX-TL. Unlike traditional testing methods reliant on plasmids, the 4–8 h benchmark provided by our method is theoretically

independent of the number of components tested. For example, to initially test an n -piece circuit *in vivo* would require $\log_3(n)$ rounds of plasmid cloning, assuming assemblies of 5 units at the same time (four regulatory units plus a vector backbone) (Figure 7a, b). This restriction results from the

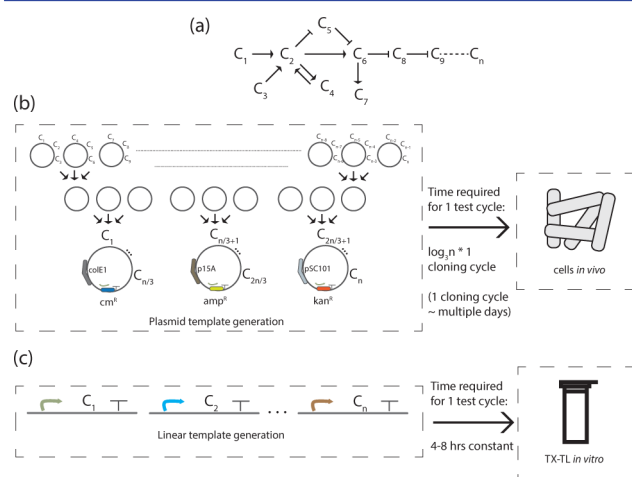


Figure 7. Linear DNA prototyping of large synthetic circuits in TX-TL. (a) A large circuit composed of n components is to be prototyped *in vivo* or in TX-TL. (b) Prototyping *in vivo* requires the reduction of n components to 3 plasmids, which can then be transformed into a cell. (c) Prototyping using rapid assembly of linear DNA requires 4–8 h, as each component can be assembled and tested in parallel.

carrying capacity of the cell to maintain a limited number of antibiotic cassettes and origins of replication. However, an initial testing cycle in TX-TL on linear DNA would require only the theoretical 8 h, as each construct can be assembled in parallel on linear DNA and immediately tested (Figure 7c). The only restriction would be the resource carrying capacity of the TX-TL reaction. However, large-scale circuit prototyping is limited by the current lack of relatively large synthetic circuits; to our knowledge, the largest currently published circuit is an 11-piece logic gate.³⁷ Once rapid assembly is established, a larger bottleneck may be the difficulty of formulating and testing novel synthetic circuits with useful function.

To reach the theoretical 8-h limit for large circuits, the rapid assembly procedure could be automated using robotics with simple pipetting and thermo-cycling capability, as the assemblies rely on standard parts, the final part is PCR amplified, and the resulting part is added to a constant-temperature TX-TL reaction. Unlike traditional methods of testing circuits, there are no cell growth, plasmid miniprep, or centrifugation steps. We have not yet explored automation of the rapid assembly procedure.

Conclusion. In this paper, we described a rapid prototyping procedure for genetic circuits utilizing linear DNA in an *E. coli* TX-TL cell-free system. This was done by characterizing methods of protecting linear DNA, and differences in gene expression between linear and plasmid DNA templates. A rapid assembly procedure entirely *in vitro* was developed, which produced results from standard parts in under 8 h. For a genetic switch, circuits on linear DNA qualitatively matched circuits on plasmid DNA. Prototyping with linear DNA in TX-TL can decrease cycle times and increase iteration speed.

We demonstrated that linear DNA results could be mapped to plasmid DNA results in the context of individual promoters. However, in the context of circuit design the mapping becomes

more complex due to multiple interconnecting relationships. While we saw expected relative circuit behavior for a genetic switch on both linear DNA and plasmid DNA, we did not attempt to map results from one mode of prototyping to the other. Such mapping may require computational toolboxes using parameters such as promoter strength and binding coefficients derived in this work.³⁸ Additionally, one would need increased understanding of experimental variation in TX-TL. For example, with plasmid DNA we have noticed expression differences dependent on the strain used for amplification, and with linear DNA expression differences between samples that were not processed in the same batch. Part of the difference is explained by exogenous steps, such as salt content postminiprep using different columns.¹⁴ We hypothesize other differences may be intrinsic to the DNA used, either through biochemical modifications or through conformational differences which have been shown *in vivo* to affect gene expression.³⁹ Some variation can be compensated for by controls, such as harvesting all plasmid DNA used in a single batch. Such approaches are analogous to those addressing ubiquitous variation in *in vivo* systems.²⁹

Ultimately, one would like to prototype circuits in TX-TL or a comparable *in vitro* environment for functionality *in vivo*. This could be challenging in light of the lack of correlation of results *in vivo* to those of TX-TL plasmid DNA data in our data set. While promoter strengths could be calibrated individually between TX-TL and *in vivo*, it is unclear how to (or if it is necessary to) calibrate complex circuits with multiple interconnecting relationships. Encouragingly, there are examples of circuits prototyped *in vitro* for *in vivo* demonstration—namely a negative feedback gene and a logic gate.^{40,41} Future work can focus on important parameters in the transition, and on the transition of complex circuits of three or more promoters or those not based on known *in vivo* motifs.

In vitro systems in general and TX-TL in specific form a strong basis for the testing of novel circuits. For applications using T7 promoters or for simple assays, finely controlled T7-based reconstituted systems without linear DNA degradation can be used.¹² However, TX-TL and S30 based systems have the additional ability to strongly express σ -70 and alternate σ -promoters, as well as provide nucleic acid degradation. There is also a wealth of data from previous S30 extract studies and from recent studies allowing for long-term expression,⁴² small-scale expression,^{43,44} and novel control techniques.⁴⁵ Rapid prototyping techniques explored in this work, when tied into other existing technologies and to characterization research, are a compelling and rapid alternative to *in vivo* systems for circuit design and testing.

METHODS

Cell-Free Expression Preparation and Execution.

Preparation of the cell-free TX-TL expression system was done according to previously described protocols, resulting in extract with conditions: 8.9–9.9 mg/mL protein, 4.5–10.5 mM Mg-glutamate, 40–160 mM K-glutamate, 0.33–3.33 mM DTT, 1.5 mM each amino acid except leucine, 1.25 mM leucine, 50 mM HEPES, 1.5 mM ATP and GTP, 0.9 mM CTP and UTP, 0.2 mg/mL tRNA, 0.26 mM CoA, 0.33 mM NAD, 0.75 mM cAMP, 0.068 mM folic acid, 1 mM spermidine, 30 mM 3-PGA, 2% PEG-8000.¹⁴ Unless otherwise specified, one extract set “eZS1” was used consistently throughout the experiments to prevent variation from batch to batch. Extract “e10” was similarly prepared for toxicity assays. Extract “e13” was

prepared using above conditions but grew only at 29 °C with a 12-h second incubation. TX-TL reactions were conducted in a volume of 10 μ L in a 384-well plate (Nunc) at 29 °C, using a three tube system: extract, buffer, and DNA. When possible, inducers such as IPTG or purified proteins such as gamS were added to a mix of extract and buffer to ensure uniform distribution. For deGFP, samples were read in a Synergy H1 plate reader (Biotek) using settings for excitation/emission: 485 nm/525 nm, gain 61. For deCFP, settings were 440 nm/480 nm, gain 61. All samples were read in the same plate reader, and for deGFP rfu units were converted to μ M of protein using a purified deGFP-His6 standard. Unless otherwise stated, end point measurements are after 8 h of expression at 29 °C.

GamS Protein Purification. The composition of buffers used was as follows: buffer L, 50 mM Tris-Cl pH 8, 500 mM NaCl, 5 mM imidazole, 0.1% Triton X; buffer W, 50 mM Tris-Cl pH 8, 500 mM NaCl, 25 mM imidazole; buffer E, 50 mM Tris-Cl pH 8, 500 mM NaCl, 250 mM imidazole; buffer S, 50 mM Tris-Cl pH 7.5, 100 mM NaCl, 1 mM DTT, 1 mM EDTA, 2% DMSO. A frozen stock of P_{araBAD}-gamS in a BL21-DE3 *E. coli* strain was grown overnight in LB-carbenicillin media. 100 mL was used to inoculate 1 L LB-carbenicillin to an OD 600 nm of 0.4–0.6 at 37 °C, 220 rpm. Cells were then incubated to 0.25% arabinose (final concentration) and grown for four additional hours at 25 °C, 220 rpm, before being pelleted and frozen at –80 °C. Cells were resuspended in buffer L, mechanically lysed and incubated with Ni-NTA agarose (Qiagen). Ni-NTA agarose was washed twice with 15 column volumes of buffer W and eluted in buffer E. Fractions with a ~13 kD band were concentrated and dialyzed into buffer S overnight and further purified on a 26/60 Sephadex 75 column. Protein concentration was verified by Bradford, concentrated to 3 mg/mL using an Ultra-0.5 3K MWCO Centrifugal Filter (Ambion), and stored in buffer S at –80 °C. Protein purity was verified by gel. Purification steps were verified by SDS-PAGE gel electrophoresis.

Plasmid DNA and PCR Product Preparation. Plasmids used in this study were constructed using standard cloning procedures and maintained in a KL740 strain if using an OR2-OR1 promoter (29 °C), a MG165S21 strain if using a Pl-tetO1 or Pl-lacO1 promoter, a BL21-DE3 strain for protein purification, a BL21 strain for promoter characterization, or a JM109 strain for all other constructs. KL740 upregulates a temperature sensitive lambda cI repressor, and MG165S21 upregulates tetR and lacI. PCR products were amplified using Pfu Phusion Polymerase (New England Biolabs) for all constructs except for those labeled with AlexaFluor-588-5-dUTP, which used Taq Polymerase (New England Biolabs), and were DpnI digested. Plasmids were either miniprepmed using a PureYield column (Promega) or midiprepmed using a NucleoBond Xtra Midi column (Macherey-Nagel). All plasmids were processed at stationary phase. Before use in the cell-free reaction, both plasmids and PCR products underwent an additional PCR purification step using a QiaQuick column (Qiagen), which removed excess salt detrimental to TX-TL, and were eluted and stored in 10 mM Tris-Cl solution, pH 8.5 at 4 °C for short-term storage and –20 °C for long-term storage.

Sequences Used for Steric Protection. Three sets of sequences were used for steric protection assays. One set was based on the vector backbone of previously published pBEST-OR2-OR1-Pr-UTR1-deGFP-T500 (Addgene #40019). Another

set, used only in Figure 2d and referred to as “Sequence 2”, was derived from the coding sequence of *gltB* and *lhr*. These sequences were found by parsing the NCBI GenBank MG1655 record in BioPython for all known coding sequences and sorting by size. A final set, used in Figure 4, was based on the vector backbone of pBEST-p15A-OR2-OR1-Pr-UTR1-deGFP-T500. Sequences were analyzed using Geneious 6.0 (Biomatters Ltd.).

In Vitro Linear DNA Assembly. Linear DNA fragments were amplified using Pfu Phusion Polymerase (New England Biolabs), DpnI digested for 5 min at 37 °C (New England Biolabs) while verified with agarose gel electrophoresis, and PCR purified using previously described procedures. Fragments were then assembled *in vitro* using either isothermal assembly or Golden Gate assembly. For isothermal assembly, Gibson Assembly Master Mix (New England Biolabs) was used according to manufacturer instructions with 1:3 molar ratio vector/insert, and reacted at 1 h at 50 °C.² For Golden Gate assembly, a 15 μ L reaction was set up consisting of equimolar amounts of vector and insert, 1.5 μ L 10 \times NEB T4 Buffer (New England Biolabs), 1.5 μ L 10 \times BSA (New England Biolabs), 1 μ L BsaI (New England Biolabs), and 1 μ L T4 Ligase at 2 million units/mL (New England Biolabs).³⁴ Reactions were run in a thermocycler at 10 cycles of 2 min/37 °C, 3 min/20 °C, 1 cycle 5 min/50 °C, 5 min/80 °C. For Golden Gate assembly, constructs with internal BsaI cut sites were silently mutated beforehand using a QuikChange Lightning Multi Site-Directed Mutagenesis kit (Agilent). For the Lambda Exonuclease/Exonuclease digest assay, we followed the assembly procedure up to assembly completion but using twice the amount of assembly mix. Then, a 20 μ L reaction was prepared with 12 μ L assembly product, 2 μ L 10 \times ExoI reaction buffer (New England Biolabs), 2 μ L 10 \times BSA (New England Biolabs), 0.5 μ L lambda exonuclease (New England Biolabs), 0.5 μ L Exonuclease I (New England Biolabs), and 3 μ L water. The control was not digested. Reaction was run for 1 h at 37 °C and PCR purified using previously described procedures.

Rapid Assembly Product Protocol. The *in vitro* linear DNA assembly protocol was followed. Overlap primers were then designed to bind over the vector:promoter and vector/terminator junctions such that while the T_m of the final primer was above 60 °C, the T_m of binding on each junction side was below 40 °C. Then, 1 μ L of the resulting assembly product was PCR amplified for 35 cycles in a 50 μ L PCR reaction, and verified by agarose gel electrophoresis. If the resulting band was 80% or more pure, the DNA was PCR purified using previously described procedures and used directly in TX-TL. Simultaneously, 2 μ L of the assembly product was transformed into cells using standard chemically competent or electrically competent procedures. The cells were grown, miniprepmed, and sequenced. PCR products off of the resulting plasmids were used as a positive control.

Linear DNA Degradation Assay. To form linear DNA with AlexaFluor distributed on the dUTP, template DNA producing deGFP was amplified using a Taq Polymerase (New England Biolabs) and AlexaFluor-594-5-dUTP (Invitrogen) according to manufacturer standards with a 1:3:4:4:4 ratio of AlexaFluor-5-dUTP/dTTP/dCTP/dATP/dGTP (New England Biolabs), DpnI digested, and PCR purified using previously described procedures. Successful labeling was verified through comparison of prestained and SybrSafe poststained agarose gel electrophoresis (Invitrogen). To form linear DNA with AlexaFluor on the 5' end, AlexaFluor 594 was

covalently linked on the 5' end to both forward and reverse synthetic primers (Integrated DNA Technologies) and used for PCR amplification. For the 2 nM assay, DNA was then added to a 105 μL TX-TL reaction in triplicate with or without gamS protein, and incubated at 29 °C. A negative control with no DNA was done in parallel. Aliquots of 10 μL were removed at indicated time points and immediately added to 50 μL of PB buffer (Qiagen) and flash-frozen in liquid nitrogen. In parallel, 2 μL of sample was read for deGFP fluorescence on a Synergy H1 Take3 Plate (Biotek). After all samples were collected, samples were PCR-purified to remove degraded components and measured on a 384-well plate (Nunc) using setting excitation/emission: 590 nm/617 nm, gain 100. Negative control values were subtracted per data point. GFP signal was normalized to end point fluorescence and AlexaFluor-594 signal was normalized to DNA present at time 0. For the 250 ng assay, similar procedures were followed except 20 nM of DNA was added to 40 μL TX-TL reactions for each condition in triplicate and aliquots of 5 μL were removed and added to 25 μL of PB buffer (Qiagen).

In Vivo Promoter Characterization. Twelve promoters and a random control sequence of DNA were cloned in front of UTR1-deGFP-T500 on a p15A low copy plasmid using standard cloning procedures and propagated at 29 °C in BL21 *E. coli* (New England Biolabs). Growth at 37 °C or cloning on a high-copy colE1 plasmid resulted in a significant mutation rate. Single colonies were simultaneously sequenced and mixed with glycerol for storage at -80 °C. Specific sequences can be found in Supporting Information S2. Frozen stocks were used to inoculate 300 mL of culture in MOPS-glycerol-carbenicillin media (MOPS EZ Rich Defined Medium Kit, Teknova, using 0.4% glycerol working concentration in lieu of glucose and adding 100 $\mu\text{g}/\text{mL}$ of carbenicillin) in a 96 DeepWell polypropylene plate (Fisher Scientific). The Pl-lacO1 sample was grown with 0.5 mM of IPTG in addition. Plate was covered with a BreatheEasy gas-permeable membrane (Sigma-Aldrich) and grown overnight at 29 °C on a Symphony Incubating Microplate Shaker (VWR), shaking at 900 rpm. Cultures were then diluted 1:50 in triplicate, grown for 4 h at 29 °C, and diluted to an OD 600 nm of 0.1–0.2 in triplicate depending on growth rate. Cultures were then grown for 90 min at 29 °C, and transferred to a CulturPlate 96-well plate (PerkinElmer) for OD 600 nm and fluorescent measurement at excitation/emission 485 nm/520 nm on a Synergy H1 plate reader. Background fluorescence from media was subtracted, and each sample was normalized to OD 600 nm. The normalized value for the random control was then subtracted. Each sample was then normalized to J23101.

TX-TL Promoter Characterization on Linear and Plasmid DNA. Sequenced cultures from frozen stocks were used to inoculate 20 mL of LB-carbenicillin media and grown in parallel to stationary phase. For each sample, 4 \times 3 mL of sample was miniprep using previously described procedures. The miniprep products were PCR purified into one 30 μL sample, and resequenced. To generate linear DNA for each sample with 250 bp of noncoding DNA at each end, the resulting plasmid was PCR amplified in 4 \times 50 μL reactions, DpnI digested, and PCR purified into one 30 μL sample. Plasmid and linear DNA were quantified by spectrophotometry. For each promoter, DNA was diluted 1:2 from 4 to 32 nM for linear DNA or 2–6 nM for plasmid DNA in water or 0.5 mM IPTG for Pl-lacO1. To generate relative strength to J23101, background fluorescence and random control sequence

fluorescence was subtracted per promoter sample, and end point data was normalized to J23101. To generate saturation curves, background fluorescence was subtracted per promoter sample, and correlation and slope for each promoter (including the random control sequence) was determined.

TX-TL Promoter Induction Curves. DNA was prepared as previously mentioned. For Pl-lacO1, 1 nM of a Pl-tetO1-lacI plasmid and 2 nM of either linear or plasmid Pl-lacO1-deGFP were combined with varying amounts of IPTG in the presence of gamS and end point fluorescence was read. For Pl-tetO1, the same was done but with 1 nM of a Pl-lacO1-tetR plasmid, 2 nM of either linear or plasmid Pl-tetO1-deGFP, and 0.5 mM of IPTG in addition to aTc and gamS to inactivate any lacI present in the extract. Data was subtracted from background fluorescence for those containing aTc.

■ ASSOCIATED CONTENT

📄 Supporting Information

Additional text, tables, and figures referenced in this article. This material is available free of charge via the Internet at <http://pubs.acs.org>.

■ AUTHOR INFORMATION

Corresponding Author

*E-mail: zsun@caltech.edu.

Author Contributions

Z.Z.S., E.Y., and C.A.H. designed the experiments with guidance from V.N. and R.M.M. Z.Z.S. performed the experiments. All analyzed the data. Z.Z.S. wrote the manuscript.

Notes

The authors declare no competing financial interest.

■ ACKNOWLEDGMENTS

We thank Shaobin Guo, Dan Siegal-Gaskins, Anu Thubagere, Jongmin Kim, and Patrik Lundin for assistance testing initial methods of linear DNA assembly and protection, Emmanuel de Los Santos for advice on protein purification, Victoria Hsiao for assistance on *in vivo* assays, Angela Ho and Jost Vielmetter for protein purification through the Caltech Protein Expression Center and contribution of Supporting Information Figure S3a, and Clare Chen and Barclay Lee for assistance in the early stages of the project. This material is based upon work supported in part by the Defense Advanced Research Projects Agency (DARPA/MTO) Living Foundries program, contract number HR0011-12-C-0065 (DARPA/CMO). Z.Z.S. is also supported by a UCLA/Caltech Medical Scientist Training Program fellowship, and Z.Z.S. and E.Y. are supported by National Defense Science and Engineering Graduate fellowships. The views and conclusions contained in this document are those of the authors and should not be interpreted as representing official policies, either expressly or implied, of the Defense Advanced Research Projects Agency or the U.S. Government.

■ REFERENCES

- (1) Green, M. R., Sambrook, J., and Sambrook, J. (2012) *Molecular Cloning: A Laboratory Manual*, 4th ed., Cold Spring Harbor Laboratory Press, Cold Spring Harbor, NY.
- (2) Gibson, D. G., Young, L., Chuang, R. Y., Venter, J. C., Hutchison, C. A., 3rd, and Smith, H. O. (2009) Enzymatic assembly of DNA molecules up to several hundred kilobases. *Nat. Methods* 6, 343–345.
- (3) Alzari, P. M., Berglund, H., Berrow, N. S., Blagova, E., Busso, D., Cambillau, C., Campanacci, V., Christodoulou, E., Eiler, S., Fogg, M. J.,

Folkers, G., Geerlof, A., Hart, D., Haouz, A., Herman, M. D., Macieira, S., Nordlund, P., Perrakis, A., Quevillon-Cheruel, S., Tarandeu, F., van Tilbeurgh, H., Unger, T., Luna-Vargas, M. P., Velarde, M., Willmanns, M., and Owens, R. J. (2006) Implementation of semi-automated cloning and prokaryotic expression screening: the impact of SPINE. *Acta Crystallogr. Sect. D* 62, 1103–1113.

(4) Ro, D. K., Paradise, E. M., Ouellet, M., Fisher, K. J., Newman, K. L., Ndungu, J. M., Ho, K. A., Eachus, R. A., Ham, T. S., Kirby, J., Chang, M. C., Withers, S. T., Shiba, Y., Sarpong, R., and Keasling, J. D. (2006) Production of the antimalarial drug precursor artemisinic acid in engineered yeast. *Nature* 440, 940–943.

(5) Kwok, R. (2010) Five hard truths for synthetic biology. *Nature* 463, 288–290.

(6) Forster, A. C., and Church, G. M. (2007) Synthetic biology projects *in vitro*. *Genome Res.* 17, 1–6.

(7) Noireaux, V., Bar-Ziv, R., and Libchaber, A. (2003) Principles of cell-free genetic circuit assembly. *Proc. Natl. Acad. Sci. U.S.A.* 100, 12672–12677.

(8) Hockenberry, A. J., and Jewett, M. C. (2012) Synthetic *in vitro* circuits. *Curr. Opin. Chem. Biol.* 16, 253–259.

(9) Kim, J., White, K. S., and Winfree, E. (2006) Construction of an *in vitro* bistable circuit from synthetic transcriptional switches. *Molecular Systems Biology* 2, 68.

(10) Kim, J., and Winfree, E. (2011) Synthetic *in vitro* transcriptional oscillators. *Molecular Systems Biology* 7, 465.

(11) Saito, H., Kobayashi, T., Hara, T., Fujita, Y., Hayashi, K., Furushima, R., and Inoue, T. (2010) Synthetic translational regulation by an L7Ae-kink-turn RNP switch. *Nat. Chem. Biol.* 6, 71–78.

(12) Shimizu, Y., Inoue, A., Tomari, Y., Suzuki, T., Yokogawa, T., Nishikawa, K., and Ueda, T. (2001) Cell-free translation reconstituted with purified components. *Nat. Biotechnol.* 19, 751–755.

(13) Nirenberg, M. W., and Matthaei, J. H. (1961) The dependence of cell-free protein synthesis in *E. coli* upon naturally occurring or synthetic polyribonucleotides. *Proc. Natl. Acad. Sci. U.S.A.* 47, 1588–1602.

(14) Sun, Z. Z., Hayes, C. A., Shin, J., Caschera, F., Murray, R. M., and Noireaux, V. (2013) Protocols for implementing an *Escherichia coli* based TX-TL cell-free expression system for synthetic biology. *J. Visualized Exp.*, e50762.

(15) Shin, J., and Noireaux, V. (2010) Study of messenger RNA inactivation and protein degradation in an *Escherichia coli* cell-free expression system. *J. Biol. Eng.* 4, 9.

(16) Shin, J., and Noireaux, V. (2010) Efficient cell-free expression with the endogenous *E. coli* RNA polymerase and sigma factor 70. *J. Biol. Eng.* 4, 8.

(17) Karzbrun, E., Shin, J., Bar-Ziv, R. H., and Noireaux, V. (2011) Coarse-grained dynamics of protein synthesis in a cell-free system. *Physical review letters* 106, 048104.

(18) Shin, J., and Noireaux, V. (2012) An *E. coli* cell-free expression toolbox: Application to synthetic gene circuits and artificial cells. *ACS Synth. Biol.* 1, 29–41.

(19) Shin, J., Jardine, P., and Noireaux, V. (2012) Genome replication, synthesis, and assembly of the bacteriophage T7 in a single cell-free reaction. *ACS Synth. Biol.* 1, 408–413.

(20) Murphy, K. C. (1991) Lambda Gam protein inhibits the helicase and chi-stimulated recombination activities of *Escherichia coli* RecBCD enzyme. *J. Bacteriol.* 173, 5808–5821.

(21) Sitaraman, K., Esposito, D., Klarmann, G., Le Grice, S. F., Hartley, J. L., and Chatterjee, D. K. (2004) A novel cell-free protein synthesis system. *J. Biotechnol.* 110, 257–263.

(22) Chappell, J., Jensen, K., and Freemont, P. S. (2013) Validation of an entirely *in vitro* approach for rapid prototyping of DNA regulatory elements for synthetic biology. *Nucleic Acids Res.* 41, 3471–3481.

(23) Lin, C. H., Chen, Y. C., and Pan, T. M. (2011) Quantification bias caused by plasmid DNA conformation in quantitative real-time PCR assay. *PLoS One* 6, e29101.

(24) Ott, J., and Eckstein, F. (1987) Protection of oligonucleotide primers against degradation by DNA polymerase I. *Biochemistry* 26, 8237–8241.

(25) Murphy, K. C. (2007) The lambda Gam protein inhibits RecBCD binding to dsDNA ends. *J. Mol. Biol.* 371, 19–24.

(26) Mosberg, J. A., Gregg, C. J., Lajoie, M. J., Wang, H. H., and Church, G. M. (2012) Improving lambda red genome engineering in *Escherichia coli* via rational removal of endogenous nucleases. *PLoS One* 7, e44638.

(27) Dillingham, M. S., and Kowalczykowski, S. C. (2008) RecBCD enzyme and the repair of double-stranded DNA breaks. *Microbiol. Mol. Biol. Rev.* 72, 642–671 Table of Contents.

(28) Seki, E., Matsuda, N., Yokoyama, S., and Kigawa, T. (2008) Cell-free protein synthesis system from *Escherichia coli* cells cultured at decreased temperatures improves productivity by decreasing DNA template degradation. *Anal. Biochem.* 377, 156–161.

(29) Kelly, J. R., Rubin, A. J., Davis, J. H., Ajo-Franklin, C. M., Cumbers, J., Czar, M. J., de Mora, K., Gliberman, A. L., Monie, D. D., and Endy, D. (2009) Measuring the activity of BioBrick promoters using an *in vivo* reference standard. *J. Biol. Eng.* 3, 4.

(30) Lutz, R., and Bujard, H. (1997) Independent and tight regulation of transcriptional units in *Escherichia coli* via the LacR/O, the TetR/O and AraC/I1-I2 regulatory elements. *Nucleic Acids Res.* 25, 1203–1210.

(31) Gardner, T. S., Cantor, C. R., and Collins, J. J. (2000) Construction of a genetic toggle switch in *Escherichia coli*. *Nature* 403, 339–342.

(32) Litcofsky, K. D., Afeyan, R. B., Krom, R. J., Khalil, A. S., and Collins, J. J. (2012) Iterative plug-and-play methodology for constructing and modifying synthetic gene networks. *Nature methods* 9, 1077–1080.

(33) Pachuk, C. J., Samuel, M., Zurawski, J. A., Snyder, L., Phillips, P., and Satishchandran, C. (2000) Chain reaction cloning: A one-step method for directional ligation of multiple DNA fragments. *Gene* 243, 19–25.

(34) Engler, C., Kandzia, R., and Marillonnet, S. (2008) A one pot, one step, precision cloning method with high throughput capability. *PLoS One* 3, e3647.

(35) Rosenfeld, N., Elowitz, M. B., and Alon, U. (2002) Negative autoregulation speeds the response times of transcription networks. *J. Mol. Biol.* 323, 785–793.

(36) Sarrion-Perdigones, A., Falconi, E. E., Zandalinas, S. I., Juarez, P., Fernandez-del-Carmen, A., Granell, A., and Orzaez, D. (2011) GoldenBraid: an iterative cloning system for standardized assembly of reusable genetic modules. *PLoS one* 6, e21622.

(37) Moon, T. S., Lou, C., Tamsir, A., Stanton, B. C., and Voigt, C. A. (2012) Genetic programs constructed from layered logic gates in single cells. *Nature* 491, 249–253.

(38) Tusa, Z. A., Singhal, V., Kim, J., and Murray, R. M. (2013) An *in silico* modeling toolbox for rapid prototyping of circuits in a biomolecular “breadboard” system, In *2013 Conference on Decision and Control*, IEEE, Florence, Italy.

(39) Higgins, C. F., Dorman, C. J., Stirling, D. A., Waddell, L., Booth, I. R., May, G., and Bremer, E. (1988) A physiological role for DNA supercoiling in the osmotic regulation of gene expression in *S. typhimurium* and *E. coli*. *Cell* 52, 569–584.

(40) Karig, D. K., Iyer, S., Simpson, M. L., and Doktycz, M. J. (2012) Expression optimization and synthetic gene networks in cell-free systems. *Nucleic Acids Res.* 40, 3763–3774.

(41) Iyer, S., Karig, D. K., Norred, S. E., Simpson, M. L., and Doktycz, M. J. (2013) Multi-input regulation and logic with t7 promoters in cells and cell-free systems. *PLoS One* 8, e78442.

(42) Niederholtmeyer, H., Stepanova, V., and Maerkl, S. J. (2013) Implementation of cell-free biological networks at steady state. *Proc. Natl. Acad. Sci. U.S.A.* 110, 15985–15990.

(43) Okano, T., Matsuura, T., Suzuki, H., and Yomo, T. (2013) Cell-free protein synthesis in a microchamber revealed the presence of an optimum compartment volume for high-order reactions. *ACS Synth. Biol.*, DOI: 10.1021/sb400087e.

- (44) Okano, T., Matsuura, T., Kazuta, Y., Suzuki, H., and Yomo, T. (2012) Cell-free protein synthesis from a single copy of DNA in a glass microchamber. *Lab on a Chip* 12, 2704–2711.
- (45) Iyer, S., and Doktycz, M. J. (2013) Thrombin mediated transcriptional regulation using DNA aptamers in DNA based cell free protein synthesis. *ACS Synth. Biol.*, DOI: 10.1021/sb4000756.